Use of ^{1}H Longitudinal Relaxation Times in the Solution Structure of Paramagnetic Proteins. Application to [4Fe-4S] Proteins

J. Gaspard Huber,‡ Jean-Marc Moulis,§ and Jacques Gaillard*,‡

Département de Recherche Fondamentale sur la Matière Condensée, SCIB-SCPM, and Département de Biologie Moléculaire et Structurale, Métalloprotéines, CEA-Grenoble, Grenoble, France

Received June 7, 1996; Revised Manuscript Received July 29, 1996⊗

ABSTRACT: The accuracy of the solution structures determined by NMR is often poor around paramagnetic centers because the properties of the near protons are strongly perturbed by the electronic spin. The structural information contained in the relaxation rates of these protons has been extracted here by measuring the longitudinal relaxation times with the inversion−recovery total correlation spectroscopy (IR-TOCSY) sequence based on the recovery of cross peaks. In addition to measurements with nonselective inversion−recovery for nonoverlapping signals, reliable data have been obtained for a majority of main-chain protons from *Chromatium vinosum* high-potential ferredoxin. When a small and constant contribution from diamagnetism as well as the electronic spin distribution over the [4Fe-4S] cluster are taken into account, the shortest longitudinal relaxation times depend directly on the distance separating the protons from the paramagnetic center. This indicates that electron−nuclei dipolar interactions are the most efficient relaxation mechanism for these protons. However, the expected dependence of the relaxation rates as the sixth power of the distance has to be corrected because of induced relaxation among fast relaxing protons. This approach reveals that the solution structure of the protein is significantly different from the crystal structure around Phe-48. In addition, it provides an independent confirmation of the actual electronic structure of the $[4Fe\text{-}4S]^{3+}$ cluster in the protein. The method devised in this work, which does not rely on specific enrichment, should be useful to improve the determination of NMR-derived solution structures of paramagnetic macromolecules.

NMR experiments on paramagnetic iron−sulfur proteins have been considerably developed in the recent years (Cheng & Markley, 1995; Bertini et al., 1995a). The main evolution has consisted in adapting classical 2D (Oh & Markley, 1990; Nettesheim et al., 1992; Gaillard et al., 1992; Banci et al., 1993; Teng et al., 1994) or 3D (Banci et al., 1995) experiments to the special case of fast relaxing protons in order to obtain structural information and, in some instances, reconstruct the 3D structure of proteins in solution (Banci et al., 1995; Bertini et al., 1995b,c; Pochapsky et al., 1994). Nevertheless, not all residues in the vicinity of the active center were detected, or, if detected, the correlations with fast relaxing signals were not always established. Some improvement was obtained by use of nuclei with lower gyromagnetic ratios than that of protons, such as ^{15}N, ^{13}C, or ^{2}H (Cheng et al., 1995; Li et al., 1995; Scrofani et al., 1995; Xia et al., 1995), for which the electron−nucleus interactions are reduced. Despite the strong perturbation induced by the electronic spin, the enhancement of the relaxation rates produced by the paramagnetic center is a potential source of information on the distance relationship between the considered nuclei and the paramagnetic center.

T_1 measurements have only been marginally used in the case of iron−sulfur proteins. Recently, Chae and Markley (1995) attempted to analyze ^{15}N relaxation times in a [2Fe-2S] ferredoxin. Similar studies with protons have also been carried out with a [3Fe-4S] ferredoxin (Gorst et al., 1995) and very recently with a [4Fe-4S] ferredoxin (Ciurli et al., 1996). In most instances, T_1 measurements have been restricted to those signals with large hyperfine shifts which are well separated from those situated in the diamagnetic envelope. Both dipolar and contact interactions contribute to the total relaxation, and the specific part due to each mechanism may be difficult to disentangle. For these protons, NMR shifts can also potentially be used to obtain structural information (Gochin & Roder, 1995; Banci et al., 1996), and this approach has been applied to Fe-S proteins in only a few instances (Bertini et al., 1995a; Huber at al., 1995).

However, in view of the relatively poor definition of the presently determined solution structures of Fe-S proteins around the cluster (Banci et al., 1995; Bertini et al., 1995b; Pochapsky et al., 1994), structural information contained in the relaxation times of protons is worth exploring, and the present study with *Chromatium vinosum* (*Cv*)[1] high potential ferredoxin (HiPIP) is aimed at addressing this question.

In cases where the relaxation process is dominated by electron−nuclear dipolar interaction, the detailed electronic structure of the polynuclear active site is likely to have a role in determining the relaxation properties of the protons. Each atom of the polymetallic Fe-S center, including atoms of coordinating residues, bears a fraction of the spin density

* Address correspondence to this author at DRFMC/SCIB/SCPM, CEA-Grenoble, 17 Rue des Martyrs, 38054 Grenoble Cedex 9, France. Telephone: (33) 76 88 35 98. Fax: (33) 76 88 50 90. E-mail: gaillard@drfmc.ceng.cea.fr.

‡ Département de Recherche Fondamentale sur la Matière Condensée.

§ Département de Biologie Moléculaire et Structurale.

⊗ Abstract published in *Advance ACS Abstracts,* September 1, 1996.

[1] Abbreviations: COSY, 2D correlation spectroscopy; TOCSY, total correlation spectroscopy; IR, inversion−recovery; *Cv*, *Chromatium vinosum*; HiPIP, high-potential ferredoxin.

S0006-2960(96)01354-2 CCC: $12.00

(Noodleman et al., 1995a). The distribution of the spin density is related to the nature and the strength of the interactions which occur among the iron atoms of the active site, and it is not yet clear how the spread of the density is related to the intensity of the dipolar interactions.

From various spectroscopic studies developed in the recent years, a clearer picture of the electronic structure of reduced and oxidized [4Fe-4S] clusters in HiPIP has been emerging. At the reduced level, the $S = 0$ ground spin state originates from dominant antiferromagnetic coupling between two mixed valence pairs of iron atoms, all assigned a formal $Fe^{2.5+}$ valence state (Middleton et al., 1980). At room temperature, excited states with $S \neq 0$ significantly contribute to the paramagnetism of the molecule. At the oxidized level, the $S = 1/2$ ground spin state can be described as the result of antiferromagnetic coupling between a mixed-valence pair of iron atoms (formally $Fe^{2.5+}$) and a ferric pair (Middleton et al., 1980). Other interactions, such as double exchange between the iron atoms of the mixed-valence pair, also contribute to establish the exact nature of the ground spin state and the ladder of excited states (Noodleman, 1988; Bominaar et al., 1994).

Conclusions deduced from results obtained in models compounds reveal that a $[4Fe\text{-}4S]^{3+}$ cluster, corresponding to the oxidized level of *Cv* HiPIP, may be stabilized with two different spin states $|9/2, 4, 1/2\rangle$ or $|7/2, 3, 1/2\rangle$ in which the numbers from left to right refer to the spin of the mixed-valence pair, of the ferric pair, and of the whole cluster. At each particular spin state are associated different spin densities on the iron and sulfur atoms constituting the cluster (Noodleman et al., 1995a). The relaxation properties exhibited at room temperature by the NMR spectra depend not only on the nature of the ground state but also on the populations of excited states. As a further complication, in most oxidized HiPIP investigated so far, the mixed-valence pair is not localized on a single pair of iron atoms but is distributed over two pairs sharing a common iron which keeps a formal $Fe^{2.5+}$ oxidation state in the two configurations. The iron atoms sharing the extra electron equilibrate between the formal Fe^{3+} and $Fe^{2.5+}$ oxidation states. The kinetics of this exchange are fast on the NMR time scale (Banci et al., 1993; Bertini et al., 1995d).

This paper describes measurements of the longitudinal relaxation times of protons in the two oxidation states of *Cv* HiPIP, an 85 amino acid protein whose X-ray (Carter et al., 1974) and solution structures (Banci et al., 1995; Bertini et al., 1995b) are known. The main contribution to the relaxation mechanism of the protons in close proximity of the active center has been established and used to set up conditions under which distance constraints can be implemented to determine structures of [4Fe-4S] proteins in solution. Such analysis has led us to propose a local conformational change of the protein in solution as compared to the crystalline state.

EXPERIMENTAL PROCEDURES

Sample Preparation. *Cv* HiPIP samples were purified as previously reported (Gaillard et al., 1992). The NMR samples were 6.5 mM of reduced protein in 50 mM sodium phosphate buffer at the uncorrected pH of 6.0 in D_2O/H_2O = 1/9 (v/v). The protein in the same buffer or in 20 mM potassium phosphate, pH 8.2, was oxidized with a 5-fold molar excess of potassium ferricyanide.

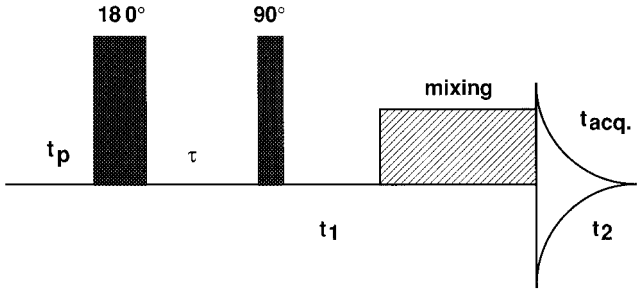

FIGURE 1: IR-TOCSY sequence. t_p, τ, and t_{acq} represent the preparation, inversion−recovery, and acquisition times, respectively.

NMR Spectroscopy. Data were recorded on a Varian 500 MHz Unity Plus spectrometer as previously described (Huber et al., 1995) at 298 K. T_1 relaxation times were measured by conventional IR pulse sequence (Bertini & Luchinat, 1986). This method is convenient for the well isolated peaks, such as hyperfine-shifted peaks. For studies on overlapping peaks, the advantage of 2D NMR spectroscopy has already been pointed out (Arseniev et al., 1986). Instead of the previously proposed IR-COSY (Arseniev et al., 1986), we have adapted the IR-TOCSY sequence (Figure 1). For paramagnetic samples with broadened lines, the cross peaks in the TOCSY sequence, which are in the pure absorption mode, are not sensitive to cancellation, unlike the antiphase signals detected with the COSY sequence. The TOCSY part of the sequence was the one already implemented (Gaillard et al., 1992). In order to limit the duration of the experiment, the IR delays (τ on Figure 1) were adapted to the T_1 range covering the characteristic relaxation times of the signals perturbed by the paramagnetism. With reduced *Cv* HiPIP, eight increments, i.e., eight IR-TOCSY experiments, were implemented with τ delays of 0, 20, 60, 90, 140, 210, 300, and 1250 ms. With oxidized *Cv* HiPIP, which is more difficult to keep over long periods, three IR-TOCSY experiments were carried out with τ delays of 0, 100, and 200 ms. Each experiment consisted in 256 increments of 2048 complex points over a spectral window of 6.5 kHz.

The majority of T_1 values were obtained by a three-parameter fit of peak intensities to the following equation (Weiss & Ferretti, 1985):

$$I(\tau) = I_0[1 - (1 + B\,(1 - \exp(-\kappa/T_1))\exp(-\tau/T_1)] \quad (1)$$

where κ is the sum of acquisition and preparation times (Figure 1), and B is an adjustable parameter which takes into account non ideal magnetization inversion and whose value is smaller than, but close to, one. This equation considers the possible partial recovery of the signal before application of the inversion pulse (Weiss & Ferretti, 1985). It reduces to

$$I(\tau) = I_0[1 - (1 + B)\exp(-\tau/T_1)]$$

when the relaxation time is much shorter than κ.

A fit using only two parameters (I_0 and T_1, with $B = 1$) was used when the intensity of the peaks was not well defined at times t much larger than T_1 and for the 2D experiments involving oxidized *Cv* HiPIP. In some instances, the null point of the IR process was used to evaluate T_1.

For the IR-COSY, it has been established that the longitudinal relaxation time of the nuclei labeled during the

evolution period (t_1, Figure 1) governs T_1 of the corresponding cross-correlation peaks (Arseniev et al., 1986). We have verified that both HN−Hα and Hα−HN cross peaks (respectively along F_1 and F_2 dimensions) generally have different relaxation times. The two experimental values correspond to the relaxation times of the HN and Hα protons. In addition, the measurements of relaxation times of several cross peaks, corresponding to correlations of, for instance, one HN proton along F_1 and several protons along F_2, are equal and apply to the amidic proton relaxation time. These duplicate measurements were important to assess the precision of the results.

The results obtained from the IR-TOCSY sequence have been compared to those obtained from normal IR sequence. The agreement between pairs of values was in the limit of expected errors for each sequence separately; for well separated peaks the difference was of the order of a few percent.

Both IR-TOCSY and the normal IR sequences give access to nonselective T_1. The consequences of the determination of nonselective T_1 have been recently discussed at length (La Mar & de Ropp, 1993). For macromolecules of intermediate size, comparable to *Cv* HiPIP, the nonselective T_1 can give an estimate of the paramagnetic contribution (T_{1par}) to the total relaxation but the T_1 extracted from an IR experiment may be meaningless for long IR delays. As pointed out by Granot (1982), if cross-relaxation is no longer negligible, the recovery of magnetization is not a monoexponential process except for very short times τ of eq 1. The validity of the single-exponential approximation has been checked here for the majority of the T_1 measurements determined by the classical IR pulse sequence and which cover a broad range of T_1 values. No significant deviation was observed between the T_1 values deduced from the slope at $\tau = 0$ and the values obtained by fitting the experimental signal amplitudes over all the IR delay range. Nevertheless, IR-TOCSY spectra have been recorded with special emphasis put on short delays.

The distances have been taken from the X-ray crystal structure of oxidized *Cv* HiPIP (Carter et al., 1974) to which the hydrogen atoms have been added by using the routine included with CHARMM (Brooks et al., 1983).

RESULTS AND DISCUSSION

Reduced HiPIP

Contributions to Relaxation. A total of 60 T_1 from cysteinyl and backbone protons has been determined by combining normal IR and IR-TOCSY experiments on the reduced protein. Although many more side chain protons could have been included, they were left aside in order to avoid introducing additional complexity arising from side chain motions.

The very short relaxation times determined in reduced *Cv* HiPIP reflect the contribution of the paramagnetic iron−sulfur center. Three terms (dipolar, contact, and curie) may contribute to the paramagnetic part of the relaxation time T_{1par}. Curie relaxation can generally be neglected (Bertini & Luchinat, 1986). An estimate of the contact contribution to T_1^{-1} gives values smaller than 0.23 s^{-1} for a proton with a chemical shift of 20 ppm (the maximum shift observed in the reduced protein) and of the order of 6 s^{-1} for a proton with a chemical shift of 100 ppm, i.e., T_1 larger than 150 ms in the range investigated here. From these estimates the dipolar contribution to T_1 seems predominant.

In order to precisely assess the dipolar contribution to T_{1par}, the fraction of spin density distributed on all atoms constituting the active site has to be considered. In magnetic coupled systems, the contribution of one metal ion is proportional to $\mu^2 D^{-6}$ (Bertini & Luchinat, 1986). Thus the dipolar contribution of a cluster to the relaxation time of a given nucleus is taken proportional to $\sum \mu_i^2 D_i^{-6}$, where the sum extends to all atoms bearing spin density μ_i, at a distance D_i from the considered proton. About 90% of the spin density is calculated to be concentrated on the iron atoms of reduced HiPIP (Noodleman et al., 1995a), and since the spin density enters the formula as its squared value, the spin density on the nonmetal atoms has only a marginal influence. Furthermore, spectroscopic evidence (Middleton et al., 1980) indicates that the four iron atoms are equivalent in the ground state of the reduced protein. A symmetric spin distribution was thus considered for the four iron atoms. It was then possible to neglect the actual value of the spin density on the iron atoms and to define a simplified reduced distance D_{red} as

$$D_{red} = (\sum D_i^{-6})^{-1/6}$$

the sum extending to all four iron atoms.[2]

At this point, it was not necessary to consider the structures determined by NMR because they are in large agreement with the crystal structure (Banci et al., 1995) and because the T_1 measurements are intended to complement and, if possible, improve the NOE data for those residues in the vicinity of the paramagnetic center.

Correlation between Relaxation Rates and Geometry. A plot of ln T_{1par} versus ln D_{red} was expected to give a straight line with a slope of six. However, when raw T_1 values were plotted, a clear divergence from a straight line was noticed which increased with D_{red}. A constant value of 0.83 s^{-1} had to be subtracted to all experimental relaxation rates in order to obtain a linear correlation over the range of D_{red} shown on Figure 2. This correction represents an average diamagnetic contribution to the relaxation times. In molecules of moderate size, the dipolar diamagnetic contribution to the relaxation rate was predicted to be compensated by cross-relaxation terms, at least for two-spin interactions (La Mar & de Ropp, 1993). Our results show that this conclusion is only qualitatively valid.

A plot of ln T_{1par} versus ln D_{min}, with D_{min} being the distance of a given proton to the closest iron, shows a dispersion along the expected straight line far larger by about 20% than when D_{red} is used. This result clearly points out that D_{red} is the most relevant and useful variable determining the relaxation rate of protons in the vicinity of $[4Fe\text{-}4S]^{2+}$ clusters.

[2] A local spin model analogous to the one recently developed by Bertrand et al. (1996) for $[4Fe\text{-}4S]^{+}$ centers could be considered. The dipolar hamiltonian is then replaced (though under restricted conditions) by an effective one in which a reduced distance is defined as $D_{red}^{-3} \approx \sum \mu_i D_i^{-3}$. The enhancement of the nuclear longitudinal relaxation is proportional to the square of the dipolar interaction between the electronic and nuclear spins, i.e., $(\sum \mu_i D_i^{-3})^2$. However, the application of such a model in the present case has not allowed us to get a better fit of the data than the use of a reduced distance as defined in the text.

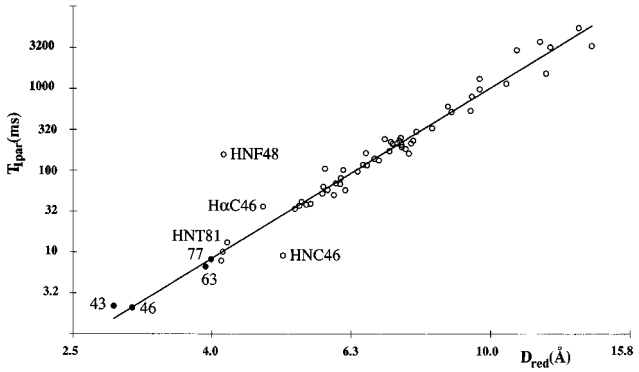

FIGURE 2: Plot of ln T_{1par} versus ln D_{red} for protons of reduced *Cv* HiPIP at pH 6.0. T_{1par} and D_{red} values were derived as stated in the text. T_{1par} of β-CH_2 cysteinyl protons are represented by ●. The line corresponds to the best fit of the data with a slope of 5.5.

The adjustment of the data of Figure 2 in the range of D_{red} for which paramagnetic relaxation is dominant gives a slope close to 5.5, i.e., significantly different from 6. Therefore, the relaxation times are shorter than expected for protons relatively far from the active site experiencing negligible contact relaxation. It is likely that the difference between the slope of Figure 2 and the theoretical value of 6 is due to the induced dipolar contribution of protons close to the iron-sulfur cluster which are interacting with protons situated further away.

The satisfactory correlation of Figure 2 clearly shows that dipolar relaxation is the dominant contribution to T_{1par}. All protons situated at D_{red} shorter than about 10 Å from the active site display signals the T_{1par} of which closely follow a dipolar law. Even the β-CH_2 of the coordinating cysteines, which experience hyperfine shifts, are mainly relaxed by dipolar interactions. Their T_{1par} are distributed on both sides of the theoretical line, with a relatively small dispersion which can in part be due to the limit of application of the point-dipole approximation for those protons very close to one iron and also by a more important contribution from the spin density on the sulfur atoms (Ciurli et al., 1996). Therefore, the hyperfine coupling of the cysteinyl protons with the $[4Fe\text{-}4S]^{2+}$ cluster is not large enough to significantly enhance the relaxation rates, in agreement with the predictions made above. For D_{red} beyond 10 Å, the dispersion of T_{1par} increases with the diamagnetic contribution to the relaxation process and the dipolar paramagnetic contribution progressively vanishes for larger D_{red}.

The equivalence of the iron atoms in $[4Fe-4S]^{2+}$ clusters is better evidenced by Mössbauer spectroscopy of the $S = 0$ spin state at low temperature (Middleton et al., 1980). The paramagnetism at ambient temperature is due to the thermal population of excited spin states with $S > 0$, $S = 1$ states being prominant among them. The correlation revealed by Figure 2 indicates that the equivalence of the four iron atoms is conserved for the excited states. This result suggests that, in a model with antiferromagnetically coupled pairs of iron atoms, the first $S = 1$ excited state is probably better described by $|9/2, 9/2, 1\rangle$ for which identical spin density on all four iron atoms is expected. This conclusion agrees with the one drawn from theoretical calculations on model compounds (J.-M. Mouesca, personal communication).

Evidence for Differences between Solution and Crystal Structures. From the NMR solution structures of *Cv* HiPIP, the conclusion that the X-ray structure of the oxidized protein satisfactorily reflects the structure of the reduced protein in solution has been deduced (Banci et al., 1995). This result is borne out by the correlation of Figure 2. However, a few data points fall significantly out of the fit of Figure 2. The two main chain protons of Cys-46 are not very well aligned with the other points of Figure 2. In the X-ray structure the amide proton is closer to the proximal iron than the Hα (Carter et al., 1974). In contrast, the T_1 measurements reported here are in better agreement with the reverse assignment. Nevertheless, these deviations from the fit in Figure 2 are smaller than the one exhibited by the unambiguously assigned HN of Phe-48 (Gaillard et al., 1992; Banci et al., 1995; Li et al., 1995). This residue displays RMSD values three times larger than average in the solution structures of the protein (Banci et al., 1995), mainly because of insufficient interresidue correlations. From the X-ray structure (Carter et al., 1974), its amidic proton should form a hydrogen bond with the sulfur atom of Cys-46. However, the corresponding T_{1par} is longer than expected from dipolar relaxation which excludes the involvement of additional contact relaxation mediated by the hydrogen bond. For instance, the HN of Thr-81, which is also predicted to form a hydrogen bond with a cysteinyl sulfur (Carter et al., 1974), displays a relaxation time one order of magnitude shorter than the HN of Phe-48 with a similar reduced distance to the cluster (Figure 2). The relaxation time of one nonstereospecifically assigned β-CH_2 proton of Phe-48 was also longer than expected. These data are suggestive of a discrepancy between the model refined from X-ray data and the structure in solution. Similar deviations from the predicted behavior have been looked for in nearby residues, but neither Gln-47 nor Gln-50 (the main chain protons of Met-49 have not been detected) display unexpected relaxation rates for their main chain protons. Therefore, the discrepancy is limited to Phe-48 (and maybe Met-49). Interestingly, molecular simulations carried out with the restraints deduced from NOE obtained from NMR data provided two sets of configurations for this region (Banci et al., 1995). One (found in roughly half of the calculated models) closely follows the structure derived from X-ray diffraction data. In contrast, the second set puts HN of Phe-48 at a reduced distance of about 6.5 Å from the cluster (instead of ca. 4 Å for the first set), i.e., where it is expected to be from T_1 measurements (Figure 2). The differences between these two sets lie in ca. 140° increases of the φ angles of residues 48 and 49 and ca. 90° decrease in ψ of Phe-48. The simplest explanation for this observation is that the two conformations of the main chain around Phe-48 can be stabilized: the crystallization conditions seem to select one of them in which the main chain is close to the [4Fe-4S] center while the second conformation is the major one in solution. The differences are illustrated in Figure 3.

Oxidized HiPIP

An analogous series of measurements was carried out for the oxidized protein. In this case, T_1 have been measured for 70 protons. But only 33 main chain protons were kept for analysis as their T_1 belong to the range for which the relaxation is dominated by the paramagnetism of the $[4Fe\text{-}4S]^{3+}$ center. *Cv* HiPIP is a protein with a relatively high (ca. 320−350 mV) oxidation potential (Moulis et al., 1988, 1993). Solutions of oxidized protein have a tendency to convert slowly to the reduced form over the long time

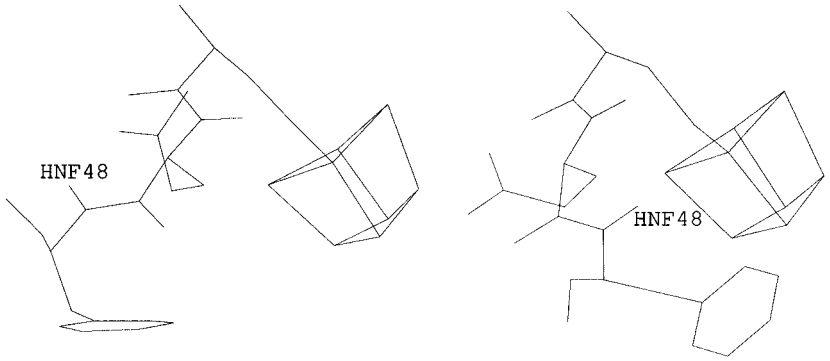

FIGURE 3: Two possible conformations of Phe-48. (Left) Representative conformation from the set of NMR structures (Banci et al., 1995) which deviates from the crystal structure but is in agreement with relaxation data presented here. (Right) Partial view of the structure obtained from X-ray data (Carter et al., 1974).

required for IR-TOCSY experiments. Since the occurrence of electron self-exchange in mixtures of oxidized and reduced proteins introduces additional relaxation pathways, it was of the utmost importance to monitor the completeness of the oxidation through the intensities of the corresponding signals. This procedure has limited the number of IR delays to only three in different IR-TOCSY experiments recorded between pH 6.0 and 8.2.

Although the oxidized protein has a paramagnetic ground state, the T_1 of its protons are longer than for the reduced protein. Such an increase is due to the overall increase in the ferric character of the cluster involving both the electronic relaxation time of the ground state and the contribution of the excited states. In the oxidized protein, the excited states probably have a smaller contribution than in the reduced protein since they are expected to lie at higher energies. Indeed, the spin ladder depends on the exchange coupling J which is larger for $[4Fe\text{-}4S]^{3+}$ clusters than for reduced ones (Noodleman et al., 1995a).

Distance Dependence of the Relaxation Rates. The same procedure described above for the reduced case was employed to extract the paramagnetic contribution T_{1par} of T_1: the measured relaxation rates were corrected by the same constant factor (0.83 s^{-1}) as above in order to take into account the diamagnetic contribution.

Experimental data on proteins (Middleton et al., 1980) and model compounds (Mouesca et al., 1993) suggest that the spin density is not equally distributed over the four iron atoms of $[4Fe\text{-}4S]^{3+}$. We have checked that an equal distribution of the spin density on the four irons produces a poor correlation between T_{1par} and D_{red} (not shown). The thermally averaged spin-projection coefficients K_i calculated by Noodleman and co-workers (1995b) are good approximations of μ_i in the valence bond approximation (Mouesca et al., 1993). Otherwise these coefficients are proportional to μ_i by a covalency factor which is, to a good approximation, equal for the four iron atoms (~0.7: Mouesca et al., 1995). K_i values of 1.6 for $Fe^{2.5+}$ and −0.9 for Fe^{3+} have been used, and the variable $D_{red} = (\Sigma K_i^2 D_i^{-6})^{-1/6}$ has been defined.

The second important difference between $[4Fe\text{-}4S]^{2+}$ and $[4Fe\text{-}4S]^{3+}$ clusters originates from the occurrence of at least two positions of the mixed-valence pair over the cluster, as evidenced by NMR (Bertini et al., 1995a). We have considered the spin density on the interchanging irons as resulting from the averaged spin density between an iron belonging to the mixed-valence pair, with positive spin density (1.6), and an iron of the ferric pair, with negative spin density (−0.9) (Noodleman et al., 1995b). This hypothesis has induced a strong dispersion of the points on the plot since a better correlation was found when the spin density was taken as the square root of half the sum of the squared values. The plot with the latter conditions is the one shown on Figure 4. We have tested all possible coupling schemes involving two electronic configurations, i.e., two positions of the mixed-valence pair (Table 1). The scheme with the iron coordinated to the first cysteine in the sequence (Cys-43) being ferric and the iron coordinated to Cys-63

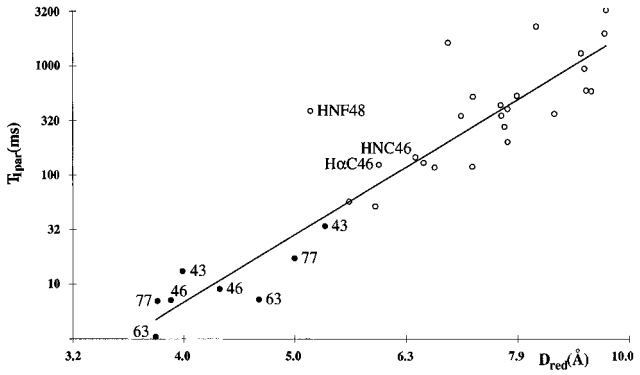

FIGURE 4: Plot of ln T_{1par} versus ln D_{red} for protons of oxidized *Cv* HiPIP at pH 8.2. T_{1par} of β-CH_2 cysteinyl protons are represented by ●. The line represents the best fit of experimental data in agreement with the electronic configuration described in row 2 of Table 1.

Table 1: Determination of the Electronic Structure of the $[4Fe\text{-}4S]^{3+}$ Cluster[a]

Fe_1	Fe_2	Fe_3	Fe_4	r
3+	2.75+	2.75+	2.5+	0.926
3+	2.75+	2.5+	2.75+	0.940
3+	2.5+	2.75+	2.75+	0.924
2.75+	3+	2.75+	2.5+	0.898
2.75+	3+	2.5+	2.75+	0.912
2.5+	3+	2.75+	2.75+	0.876
2.75+	2.75+	3+	2.5+	0.876
2.75+	2.5+	3+	2.75+	0.873
2.5+	2.75+	3+	2.75+	0.852
2.75+	2.75+	2.5+	3+	0.909
2.75+	2.5+	2.75+	3+	0.892
2.5+	2.75+	2.75+	3+	0.872

[a] The 12 possible distributions of the valence states on the four iron atoms of the oxidized cluster have been considered. Fe_1 to Fe_4 are atoms attached to Cys-43, -46, -63, and -77, respectively. The corresponding ln T_{1par} versus ln D_{red} plots were drawn for 33 (main chain and β-CH_2 cysteinyl) protons closest to the active site with the exception of the HN of Phe-48. The resulting correlation coefficients r are given.

being in the formal $Fe^{2.5+}$ valence was the one which better agreed with our results (second row of Table 1). This result is in perfect agreement with the previously established conclusion based on the chemical shifts of cysteinyl β-CH_2 protons observed in various HiPIP (Bertini et al., 1995d).

In the case of oxidized *Cv* HiPIP, the T_{1par} values are more scattered with a correlation factor of 0.94 (to be compared to a value of 0.98 in the reduced sample). This increased dispersion is largely due to the relatively small number of experiments used for T_1 measurements. It can also be noticed that the value of D_{red} for which significant deviation from the fit occurs is smaller in the case of oxidized HiPIP (ca. 8 Å, Figure 4) than in the case of reduced HiPIP (ca. 10 Å, Figure 2). This is due to the overall smaller relaxation rates measured for oxidized HiPIP and to the smaller influence of the paramagnetic contribution to the relaxation properties of protons at relatively shorter distances from the cluster.

No significant difference in the above correlation have been found when considering either of the spin states $|9/2, 4, 1/2\rangle$ and $|7/2, 3, 1/2\rangle$ proposed for oxidized HiPIP (Mouesca et al., 1993). Discriminating between these states may be possible if well established level diagrams were available. This point needs further investigation, both theoretically and experimentally, in order to improve the present analysis.

Structural Consequences. In spite of the additional sources of inaccuracy in the T_1 measurements for oxidized HiPIP, the HN of Phe-48 is again the proton which deviates most from the fit of Figure 4, as in the case of reduced HiPIP. The reason for the difference is most likely the same since the same X-ray structure has been used in both analyses: the solution structure of *Cv* HiPIP is different from the crystal structure in that the main chain HN of Phe-48 is turned away from the cluster instead of toward the sulfur of Cys-46. This result indicates that the difference between the structures in solution and in the crystal is independent of the redox level, and it will have to be considered when analyzing the properties of the protein in solution.

Another source of discrepancy concerns the β-CH_2 cysteinyl protons which experience a stronger contact relaxation. The two β-CH_2 protons of Cys-63, which have the most shifted resonances, have also relaxation rates slightly enhanced by contact relaxation.

Concluding Remarks

The range of accessible T_1 for the strongly paramagnetic *Cv* HiPIP has been extended to protons of the diamagnetic envelope by the use of the IR-TOCSY sequence. This method allows for duplicate measurements of a particular T_1 and was also used as an internal check of the consistency of the data.

The electron−nuclear dipolar contribution has been demonstrated to be the dominant mechanism to the paramagnetic relaxation times of protons of reduced *Cv* HiPIP situated at a reduced distance less than 10 Å from the cluster. The spin density equally distributed over the four iron atoms contributes to the relaxation. But the slope of the regression of ln T_{1par} as a function of the reduced distance deviates slightly from the expected sixth power law. This deviation is attributed to diffusional behavior due to the interaction of a given proton with fast relaxing protons located closer to the active site. When all the contributions to the relaxation were taken into account, only isolated T_{1par} significantly departed from the general behavior.

This study also clearly demonstrates that the T_1, when properly scaled as a function of both distances and spin densities on the metal ions, could be introduced as new structural constraints for establishing the 3D structure of [4Fe-4S] proteins in solution. This is particularly true in the vicinity of the clusters where the classical NOE constraints are less numerous, and their intensities have to be corrected to take into account the effect of the paramagnetic relaxation (Bertini et al., 1996). The most obvious use of the approach has been provided by the localized change of conformation of the main chain around Phe-48 evidenced here in solution as compared to the crystal structure.

Despite the more complex situation of the oxidized state, the dominant dipolar electron−nucleus character of the relaxation mechanism was also evidenced. A larger dispersion of the experimental data was observed but the same conclusions as for the reduced case may be extrapolated to the oxidized level. The relaxation data confirm the previously established model for the location of the ferric iron and the dynamic equilibrium of the mixed-valence pair in *Cv* HiPIP.

In view of the general rules established herein for the relaxation properties of the protons of *Cv* HiPIP, it can be anticipated that the distance relationships derived from T_1 measurements will significantly contribute to improve the future structure determination of [4Fe-4S] proteins in solution.

ACKNOWLEDGMENTS

We thank J.-M. Mouesca and L. Emsley for helpful discussions and J. Meyer for careful reading of the manuscript.

SUPPORTING INFORMATION AVAILABLE

Tables of relaxation times measured and plotted on Figures 2 and 4 for the reduced and oxidized HiPIP from *C. vinosum* with the corresponding reduced distances (2 pages). Ordering information is given on any current masthead page.

REFERENCES

Arseniev, A. S., Sobol, A. G., & Bystrov, V. F. (1986) *J. Magn. Reson. 70*, 427−435.

Banci, L., Bertini, I., Capozzi, F., Carloni, P., Ciurli, S., Luchinat, C., & Piccioli, M. (1993) *J. Am. Chem. Soc. 115*, 3431−3440.

Banci, L., Bertini, I., Dikiy, A., Kastrau, D. H. W., Luchinat, C., & Sompornpisut, P. (1995) *Biochemistry* 34, 206−219.

Banci, L., Bertini, I., Bren, K. L., Cremonini, M. A., Gray, H. B., Luchinat, C., & Turano, P. (1996) *J. Biol. Inorg. Chem. 1*, 117−126.

Bertini, I., & Luchinat, C. (1986) *NMR of Paramagnetic Molecules in Biological Systems*, The Benjamin/Cummings, Menlo Park, CA.

Bertini, I., Ciurli, S., & Luchinat, C. (1995a) *Struct. Bonding 83*, 1−54.

Bertini, I., Dikiy, A., Kastrau, D. H. W., Luchinat, C., & Sompornpisut, P. (1995b) *Biochemistry 34*, 9851−9858.

Bertini, I., Donaire, A., Feinberg, B. A., Luchinat, C., Piccioli, M., & Yuan, H. (1995c) *Eur. J. Biochem. 232*, 192−205.

Bertini, I., Capozzi, F., Eltis, L. D., Felli, I. C., Luchinat, C., & Piccioli, M. (1995d) *Inorg. Chem. 34*, 2516−2523.

Bertini, I., Felli, I. C., Luchinat, C., & Rosato, A. (1996) *Proteins 24*, 158−164.

Bertrand, P., Camensuli, P., More, C., & Guigliarelli, B. (1996) *J. Am. Chem. Soc. 118*, 1426−1434.

Bominaar, E. L., Borsch, S. A., & Girerd, J.-J. (1994) *J. Am. Chem. Soc. 116*, 5362−5372.
Brooks, B. R., Bruccoleri, R. E., Olafson, B. D., States, D. J., Swaminathan, S., & Karplus, M. (1983) *J. Comput. Chem. 4*, 187−217.
Carter, C. W., Jr., Kraut, J., Freer, S. T., Xuong, N.-H., Alden, R. A., & Bartsch, R. G. (1974) *J. Biol. Chem. 249*, 4212−4225.
Chae, Y. K., & Markley, J. L. (1995) *Biochemistry 34*, 188−193.
Cheng, H., & Markley, J. L. (1995) *Annu. Rev. Biophys. Biomol. Struct. 24*, 209−237.
Cheng, H., Westler, W. M., Xia, B., Oh, B.-H., & Markley, J. L. (1995) *Arch. Biochem. Biophys. 316*, 619−634.
Ciurli, S., Cremonini, M. A., Kofod, P., & Luchinat, C. (1996) *Eur. J. Biochem. 236*, 405−411.
Gaillard, J., Albrand, J.-P., Moulis, J.-M., & Wemmer, D. E. (1992) *Biochemistry 13*, 5632−5639.
Gorst, C. M., Yeh, Y.-H., Teng, Q., Calzolai, L., Zhou, Z.-H., Adams, M. W. W., & La Mar, G. N. (1995) *Biochemistry 34*, 600−610.
Granot, J. (1982) *J. Magn. Reson. 49*, 257−270.
Gochin, M., & Roder, H. (1995) *Protein Sci. 4*, 296−305.
Huber, J. G., Gaillard, J., & Moulis, J.-M. (1995) *Biochemistry 34*, 194−205.
La Mar, G. N., & de Ropp, J. S. (1993) in *Biological Magnetic Resonance* (Berliner, L. J., & Reuben, J., Eds.) Vol. 12, pp 1−73, Plenum Press, New York.
Li, D., Cottrell, C. E., & Cowan, J. A. (1995) *J. Protein Chem. 4*, 115−126.
Middleton, P., Dickson, D. P. E., Johnson, C. E., & Rush, J. D. (1980) *Eur. J. Biochem. 104*, 289−296.
Mouesca, J.-M., Rius, G., & Lamotte, B (1993) *J. Am. Chem. Soc. 115*, 4714−4731.
Mouesca, J.-M., Noodleman, L., Case, D. A., & Lamotte, B. (1995) *Inorg. Chem. 34*, 4347−4359.
Moulis, J.-M., Lutz, M., Gaillard, J., & Noodleman, L. (1988) *Biochemistry 27*, 8712−8719.
Moulis, J.-M., Scherrer, N., Gagnon, J., Forest, E., Pétillot, Y., & Garcia, D. (1993) *Arch. Biochem. Biophys. 305*, 186−192.
Nettesheim, D. G., Harder, S. R., Feinberg, B. A., & Otvos, J. D. (1992) *Biochemistry 31*, 1234−1244.
Noodleman, L. (1988) *Inorg. Chem. 27*, 3677−3679.
Noodlemann, L., Peng, C. Y., Case, D. A., & Mouesca, J.-M. (1995a) *Coord. Chem. Rev. 114*, 199−244.
Noodleman, L., Chen, J.-L., Case, D. A., Giori, C., Rius, G., Mouesca, J.-M., & Lamotte, B. (1995b) in *Nuclear Magnetic Resonance of Paramagnetic Macromolecules* (La Mar, G. N., Ed.) pp 339−367, NATO ASI Series, Kluwer Academic Publishers, Dordrecht, The Netherlands.
Oh, B.-H., & Markley, J. L. (1990) *Biochemistry 29*, 3993−4004.
Pochapsky, T. C., Ye, X. M., Ratnaswamy, G., & Lyons, T. A. (1994) *Biochemistry 33*, 6424−6432.
Scrofani, S. D. B., Brownlee, R. T. C., Sadek, M., & Wedd, A. G. (1995) *Inorg. Chem. 34*, 3942−3952.
Teng, Q., Zhou, Z. H., Smith, E. T., Busse, S. C., Howard, J. B., Adams, M. W. W., & La Mar, G. N. (1994) *Biochemistry 33*, 6316−6326.
Weiss, G. H., & Ferretti, J. A. (1985) *J. Magn. Reson. 61*, 490−498.
Xia, B., Westler, W. M., Cheng, H., Meyer, J., Moulis, J.-M., & Markley, J. L. (1995) *J. Am. Chem. Soc. 117*, 5347−5350.

BI961354Z